International Journal of Research in Engineering and Science (IJRES)
ISSN (Online): 2320-9364, ISSN (Print): 2320-9356
www.ijres.org Volume 4 Issue 2 ǁ Feb. 2016 ǁ PP.85-93

Study the effect of MMF stub on the sensitivity of a photonic crystal fiber

Chandrakanta Nayak, Madhulita Mohapatra, Rashmiprava Mishra
Department of Electronics and Communication Engineering, NM Institute of Engineering and Technology,Bhubaneswar , Odisha
Department of Electronics and Communication Engineering,Aryan Institute of Engineering and Technology Bhubnaeswar , Odisha
Department of Electronics and Communication Engineering,Capital Engineering College,Bhubaneswar,Odisha

ABSTRACT: *A simple photonic crystal fiber (PCF) based Mach–Zehnder interferometric sensor is reported for sensing the refractive index and level of liquid. The sensing head is formed by all-fiber in-line single mode–multi mode–photonic crystal–single mode fiber structure using the fusion splicing method. The interferometric pattern, observed in the PCF interferometer using monochromatic source and temperature sensing arrangement, is novel and reported for the first time to the best of our knowledge. The refractive index sensitivity of the interferometric device is increased by using multimode fiber. The output intensity at the end of lead-out single mode fiber decreases with increase in refractive index of surrounding. The index sensitivities of the interferometric devices are 440.32 lw/RIU, 267.48 lw/RIU and 195.36 lw/RIU with sensing length 2.10 cm, 5.50 cm and 7.20 cm respectively. A 7.20 cm longed PCF sensor exhibits liquid level sensitivities 1.032 lw/cm, 1.197 lw/cm, and 1.489 lw/cm for three different liquid respectively.*
Keywords*:Photonic crystal fiber Mach–Zehnder interferometer Fusion splicing of PCF Fiber optics sensor Finite element method*

I. INTRODUCTION

From 1890, fiber optics sensing experiment had started and today it has spread out through worldwide laboratory [1]. With prospect of optoelectronics, optical fibers have been used at vari-ous sensor fields as it has some unique characteristics such as low fabrication cost, small, robust, high accuracy, multiplexing, remote sensing, high flexibility, low propagation loss, high sensitivity, and immunity to electromagnetic interference. Now a days, fiber is utilized as temperature, strain, pressure, rotation, displacement, refractive index (RI), polarization, ultrasound, vibra-tion, viscosity, turbidity, humidity, water level etc. parameter sensors [2]. At early days fiber optics sensor fabrication was very costly. As market price of optical fiber and optical component are reducing day by day, so fiber optics sensors are now commercialized.

There are two types of fabricated Mach–Zehnder interferometer (MZI) available, one is two-arm interferometer and another is modal interferometer [3]. The advantage of modal interferometer compared to two-arm is that it reduces the susceptibility to envi-ronmental fluctuations as the modes propagate in the same path. All fiber Mach–Zehnder interferometers possess absolute response parameter, large dynamic range and high sensitivities. Recently, several types of modal MZI sensors have fabricated for sensing temperature and other parameters. A high temperature sensor has fabricated by fusion splicing of single mode fiber and multi-mode fiber by core diameter mismatch [4,5]. At lead-in splice point, mode field diameter (MFD) mismatch takes place between two fibers, hence light of core-mode couples in the cladding-mode. As a result, interference occurs at lead-out fiber by further coupling of cladding and core mode. A curvature sensor based on PCF modal interferometer with complete collapse of microholes in the PCF has introduced a high sensitivity to the curvature change [6]. The novel fiber in-line MZI with a misalignment-spliced joint has demon-strated to develop sensors which can measure tensile strain and temperature [7]. A piece of small-core photosensitive fiber (SCPSF) has spliced between two pieces of single mode fiber (SMF) to sense high temperature fiber sensor based on the modal interferometer [8]. It is proposed that moisture sensitive materials HEC/PVDF are used to form the hydrogel coating on the no-core fiber, operating based on intensity modulation has a higher RH sensitivity at 1310 nm [9].

Photonic crystal fiber is composed with array of air-holes through length. The core region of PCF is made by removing air-holes from its center. Unique properties like single mode behavior within a wide wavelength range, very large mode area, and unusual dispersion of PCF make it applicable in wide area. Pho-tonic crystal fiber is used widely as sensing probe in temperature

sensing area. MZI can be formed by fusion splicing two PCF with small lateral offset and partially collapsing the air holes at two regions in a single piece of PCF [10]. This type of interferometer is used as ultra-high temperature sensor. Beatriz Larrión et al. [11] have proposed that Quantum dot nano coating deposited at the sur-face of air holes of LMA-20 PCF by means of layer-by-layer tech-nique can sense (40 LC to 70 LC) temperature. The transmission power is used as a sensor signal for investigating the temperature properties by infiltration of liquid within air holes of PCF [12,13]. It is possible to fabricate MZI by fusion splicing between single mode fiber and photonic crystal fiber. Two collapsed points are formed at splice region because of collapsing of air holes. The gen-eration and recombination of two modes occur at these two regions [14]. The refractometry study has done by this type of interferom-eter with high resolution putting sensing length within sucrose solution. It is possible to sense the refractive index by depositing liquid over the surface of sensing length [15]. The liquid level sensor has fabricated by thinned fiber with very simple arrangement [5].

In our present study, MMF has been used in where I, between single mode and stub of PCF as it can couple the light from core to PCF cladding mode. Dn ¼ MMF–PCF and SMF–PCF have spliced by conven-tional fusion splicer. The splicing optimization conditions have set by hit and trial method for this specialty fiber. The sensor based on conventional fiber has solid core, hence there is possibility of leakage of propagated wave. Photonic crystal fiber has air-holes along length in cladding region which couple wave more than solid cladding as confinement loss is lower in PCF. The temperature sensing range has developed from 30 LC to 120 LC at 1550 nm. The intensity of output fiber has measured by detector. The differ-ent concentrations of sucrose solution have achieved for refractive indices in the range of 1.33 to 1.42. A simple set-up has also arranged for liquid level sensing of three different liquids (milk, soil, glucose mixed with water).

II. DEVICE FABRICATION AND EXPERIMENT

2.1. Fabrication of PCF interferometer

The device is designed as shown in Fig. 1, where LMA-8 PCF (NKT Photonics), MMF (50/125 lm, THORLABS), SMF patch cables are used. PCF has outer diameter 125 lm, pitch 5.6 lm and air-hole diameter 2.58 lm. A piece of PCF is fusion spliced with MMF in manual mode by SUMITOMO T-39 fusion splicer. The optimization conditions for splicing are 2 s fusion time, 0.15 s prefusion time,
10 lm arc gap, 10 lm overlap and arc power 027 level [16–18]. The unspliced ends of PCF–MMF combination are cleaved in proper length and both are spliced with SMF. The optimization conditions for PCF–SMF splicing are 0.10 s fusion time, 0.05 s prefusion time, 10 lm arc gap and 10 lm overlap 027 level arc power. MMF–PCF and PCF–SMF splice points are collapsed region, as air holes are collapsed during splicing. As a consequence, in the collapsed region there will be no cladding part, so PCF will not be single mode anymore [10]. A part of light wave from core part of MMF can couple in cladding part of PCF. The recombination of light takes place at second splice point and interference occurs at core of single mode fiber. The intensity at the end of SMF is analyzed by OSA (YOKOGAWA, AQ6370C).

A combination of single mode fiber–photonic crystal fiber– single mode fiber (SMF–PCF–SMF) is also fabricated by fusion splicing method to compare advantage of introducing MMF in designed sensing device.

2.2. Principle of interferometer

Theoretically, we can assume that intensity at the end of PCF stub of length L (which is known as sensing length of this device) is

$$I = I_1 + I_2 + 2\sqrt{I_1 I_2}\cos\frac{2\pi Dn L}{k} \quad (1)$$

and I_2 are the intensities of the two interfering modes, n_2 is the difference between effective indices of twointerfering mode.

Whenever sensing length is introduced within heat chamber, there will be variation of n_1 and n_2 due to thermo-optic effect. The length of device will change with the variation of temperature due to thermal expansion. Previous studies [19,20] have shown by Finite Element Method (FEM) that after neglecting higher order terms, phase difference depends upon temperature variation as follows:

$$Du = \frac{2pL\delta T}{n}\frac{dD}{DT}: \quad 2$$

$$\frac{k \quad dT}{} \qquad \text{ð Þ}$$

Sensitivity of the device is given by

$$S \quad \frac{Du}{LT2} \quad ¼ \quad p \quad ; \qquad \text{ð3Þ}$$

where T_{2p} is temperature difference when the phase difference is 2p. The sensing length (L) represents the length of PCF. The differ-ence of effective indices between fundamental mode and higher order mode are calculated by using FEM at different temperatures. The effective refractive index is simulated Dn (T_0) 4.057 10 ^{3} at room temperature and thermo-optic coefficient $^{d}{}_{d}{}^{D}{}_{T}{}^{n}$ is obtained as 1.2 10 ^{8} at initial temperature.

2.3. Experiment

The fabricated MZI sensors for three different length of PCF (7.20 cm, 5.50 cm, and 2.10 cm) are characterized for sensing temperature, refractive index and liquid level. Two replicas for each length of interferometer are fabricated for sensing three parameters separately. The temperature sensing experiment is conducted for interferometers associated with the length of PCF 7.20 cm, 5.50 cm, 2.10 cm, and MMF 0.4 cm at a wave-length of 1550 nm to establish interferometric nature of the devices. The temperature chamber is constructed by Mica-sheet and it is thermally stabilized for 20–30 min for each degree of cen-tigrade temperature during experiment. The sensing length is fixed inside the temperature chamber. The chamber is heated from 30 LC to 120 LC by using Nichrome heating coil wrapped around sensing length provided a uniform ambient temperature of the fiber. The

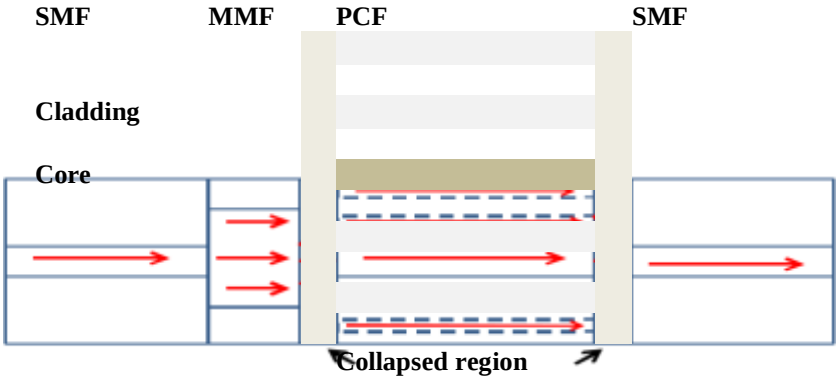

Fig. 1. Schematic diagram of the MZI sensor.

variation of transmission power versus temperature is plotted which is evidence of interferometric behavior of the device.

During refractive index (RI) measurement, sensing length is kept straight to avoid bending loss inside the refractive index chamber. The experiments are conducted with single mode fiber–multi mode fiber-photonic crystal fiber-single mode fiber (SMF–MMF–PCF–SMF) structure and SMF–PCF–SMF structure. The setup and the sample solution are maintained at constant ambient temperature. Sucrose solutions of different concentrations are prepared to create different refractive index from 1.33 to 1.42 ranges (Fig. 2).

After RI measurements the third set of SMF–MMF–PCF–SMF structure interferometers are used to sense as liquid level sensor by using three turbid medium (milk, soil, and glucose). The sensor probe is kept vertically straight within a beaker as shown in Fig. 3. A vernier caliper is arranged beside the fiber sensing length to measure liquid level.

III. RESULT AND DISCUSSIONS

3.1. Evidence of the interferometric pattern

The analytical graphical plots of transmission power versus tem-perature with different sensing length are shown in Figs. 4–6. The intensity distribution repeats after every phase change of 2p which gives sinusoidal pattern. This sinusoidal pattern explains the inter-ferometric characteristics of the sensor. Using FEM, it is found that the phase difference is 0:94p i.e. very close to p after each 5 LC tem-perature interval for 7.20 cm sensing length. The experimental results are fitted with sinusoidal curve, having equation y ¼ A_0 þ A sinðxx uÞ, where y represents transmission power and x represents temperature. The sensors have sensitivity of 0.0966

radian/LC/cm, 0.0547 radian/LC/cm, and 0.4272 radian/LC/ cm for 7.20 cm, 5.50 cm and 2.10 cm sensing length respectively.

The photonic crystal fiber interferometric sensing has conducted in broad spectrum range by various groups [3–5,10,14,15]. But we have demonstrated a device which works at monochromatic wave-length with higher accuracy. The transmission power through the device propagates in its maximum and minimum value after partic-ular temperature difference in both cases. The phase difference of wave between core and cladding mode depends upon initial length of fiber, wavelength of light and thermo-optic coefficient [20]. The thermo-optic co-efficient and length of fiber vary with temperature in such a way that phase will change periodically. Thus, the intensity of transmitted light through device becomes sinusoidal function of temperature. The sensitivity of temperature is measured by phase change in per unit length and per unit degree Celsius. The LMA-8 photonic crystal fiber is designed by FEM [21] and effective indices difference of fundamental and higher order mode is also simulated for 5 LC temperature difference (Fig. 7).

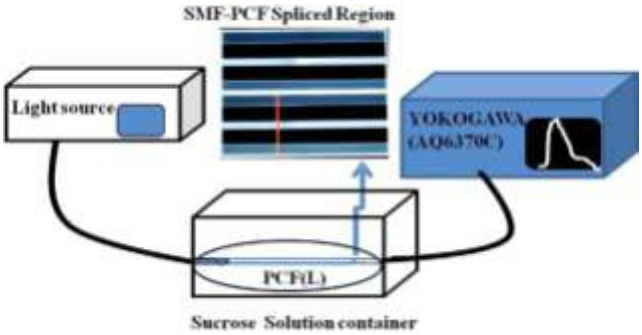

Fig. 2. Illustrate experimental set-up for refractive index sensing measurement, microscope image of spliced region between the SMF (on the left) and the PCF (on the right) shown at top.

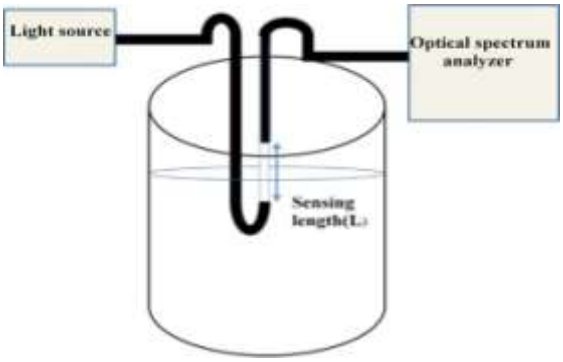

Fig. 3. Illustrate experimental set-up for liquid level sensor.

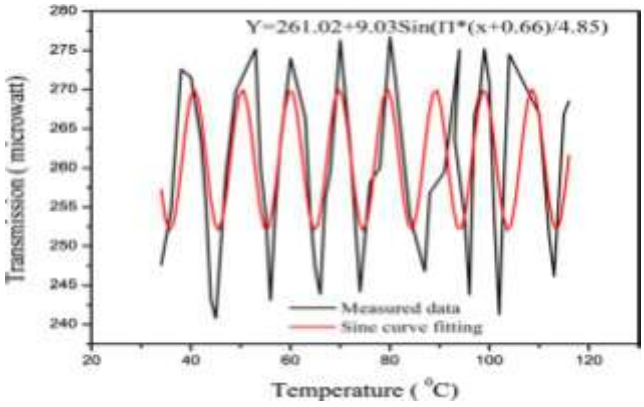

Fig. 4. Transmission power versus temperature plot at wavelength 1550 nm, with sensing length 7.20 cm.

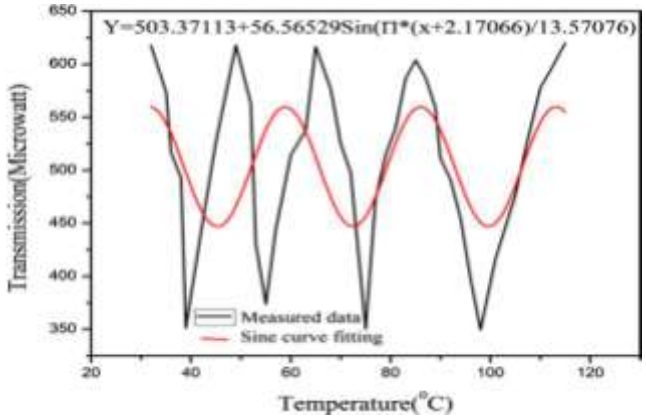

Fig. 5. Transmission power versus temperature plot at wavelength 1550 nm, with sensing length 5.50 cm.

3.2. Refractive index measurement

The response of the described sensors to the surrounding refractive index (RI) is investigated by putting the entire PCF length in sucrose solution with different concentration. MMF behaves like a mode coupler here. To explain the advantage of multimode fiber, experimental results for SMF–PCF–SMF structure and SMF–MMF–PCF–SMF structure are shown in the Figs. 8 and 9 respectively.

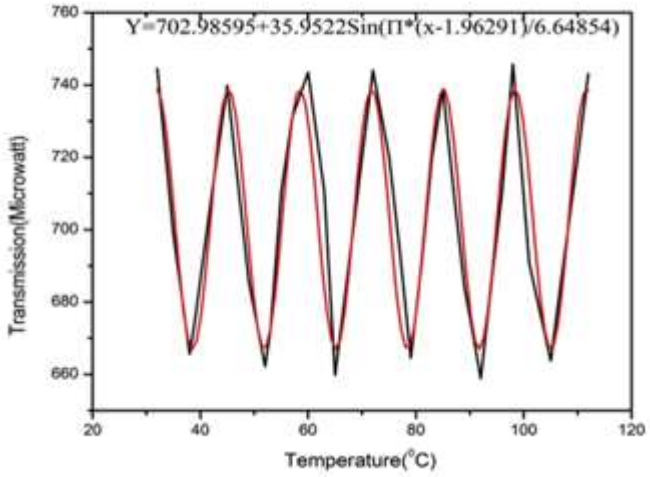

Fig. 6. Transmission power versus temperature plot at wavelength 1550 nm, with sensing length 2.10 cm.

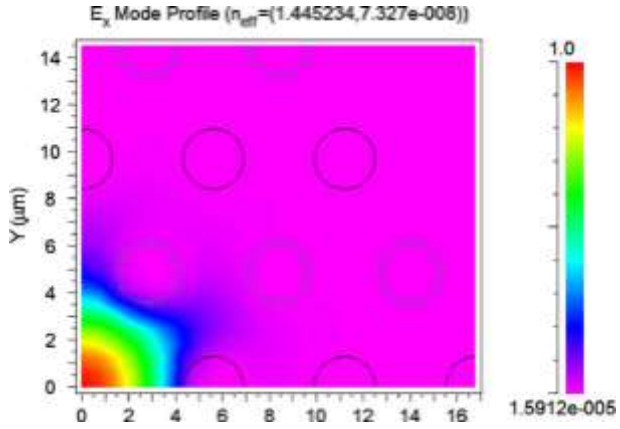

Fig. 7. The higher order mode propagation into PCF, according to FEM simulation.

SMF–PCF–SMF structure interface pattern is generated due to collapsed region at SMF and PCF spliced point. But light wave could not introduce through outer ring of holes in PCF. A maximum part of light

wave will go through core and nearer ring of hole to core of PCF and the possibility of light refraction at outer surface of PCF will decrease during index sensing. Therefore, transmission of light wave remains almost same with variation of surrounding RI. R^2 values of linear fit to the plot of transmission power versus RI of sucrose solution are less than 0.9 for two sensing lengths (L_{PCF} = 7.20 cm, L_{PCF} = 2.10 cm).

By introducing MMF, maximum part of light is coupled within core and outer ring of holes in PCF. It results in sharp decrease of transmission power with increasing surrounding RI as light will refract from lighter to denser medium. R^2 values of the linear fit graph to the plot of transmission power versus RI of sucrose solution are almost greater than 0.9 which describe the linearity of our device. Present studies demonstrate that these types of sensors with sensing length of PCF 2.10 cm, 5.50 cm, and 7.20 cm have sensitivities 440.32 lw/RIU, 267.48 lw/RIU, and 195.36 lw/ RIU respectively.

3.3. Liquid level measurement

The section of PCF is kept vertically straight within liquid. The liquid level is increased by using a burette drop by drop. The trans-mission spectrum is measured by optical spectrum analyzer with

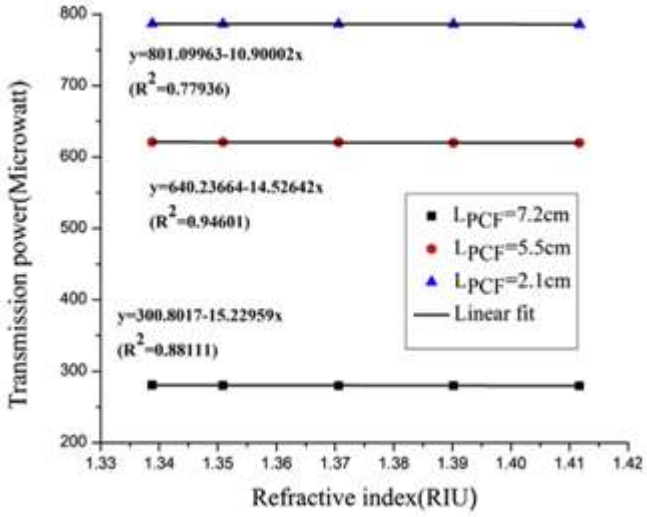

Fig. 8. Transmission power versus refractive index plots for sensing length 2.10 cm, 5.50 cm, 7.20 cm respectively with SMF–PCF–SMF structure.

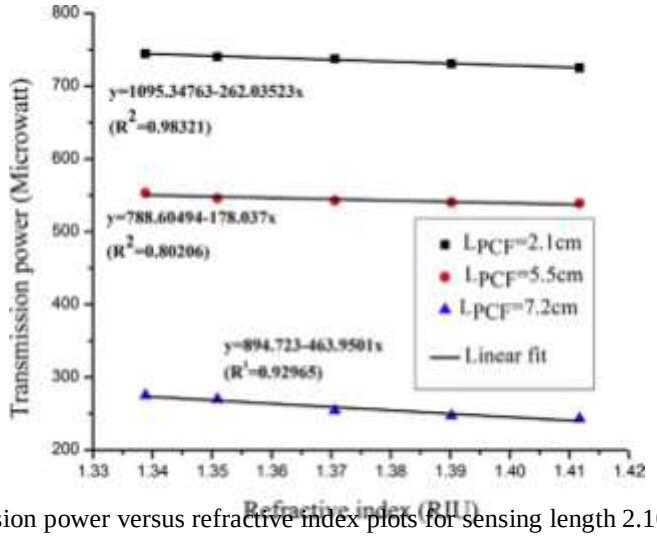

Fig. 9. Transmission power versus refractive index plots for sensing length 2.10 cm, 5.50 cm, 7.20 cm respectively with SMF–MMF–PCF–SMF structure.

rising of liquid level regularly (Fig. 3). We have used three turbid medium for verification of liquid level sensitivity of this device.

The turbidity is the cloudiness or haziness of a fluid caused by individual particles (suspended solids) that are generally invisible to the naked eye, similar to smoke in air. Many properties in a tur-bid media such as viscosity, transmittance, surface tension, density etc. can be determined by optical sensing measurements [22]. In our study, we are interested in light interaction with particles of turbid medium and absorbance of medium. Higher the turbidity, higher is the absorbance of medium. In Figs. 10–12 it is shown clearly that milk has higher absorbance than soil and glucose. We can say that our device can sense absorbance of different turbid medium. But this paper is not focused with this parameter.

When a section of PCF is surrounded by a liquid, effective refractive index of cladding mode increases but core mode almost remains unchanged which results decrease of Dn. The refraction of light wave will increase with increasing concentration of surround-ing liquid at the outer surface of PCF. If a fixed concentrated surrounding liquid level is increased, the scope of refraction of light at the outer surface of PCF increases. As the used surrounding

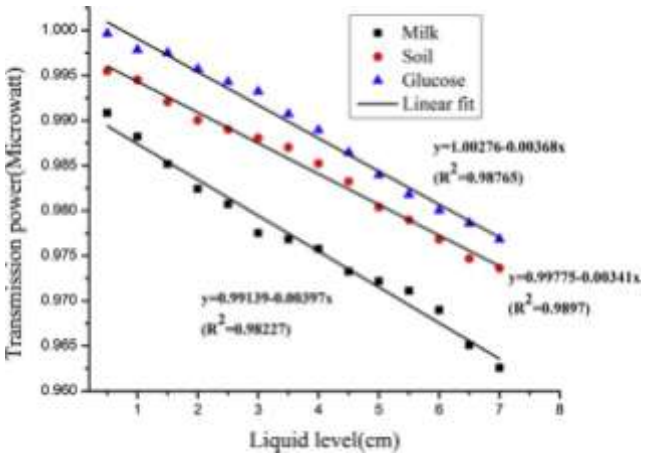

Fig. 10. Transmission power versus liquid level plot for sensing length 7.20 cm with SMF–MMF–PCF–SMF structure.

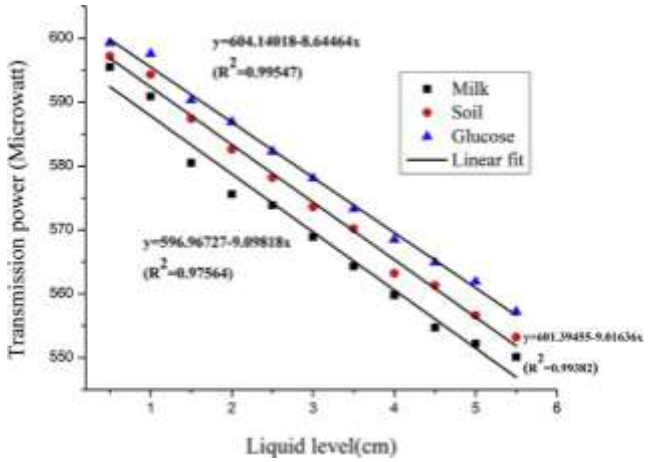

Fig. 11. Transmission power versus liquid level plot for sensing length 5.50 cm with SMF–MMF–PCF–SMF structure.

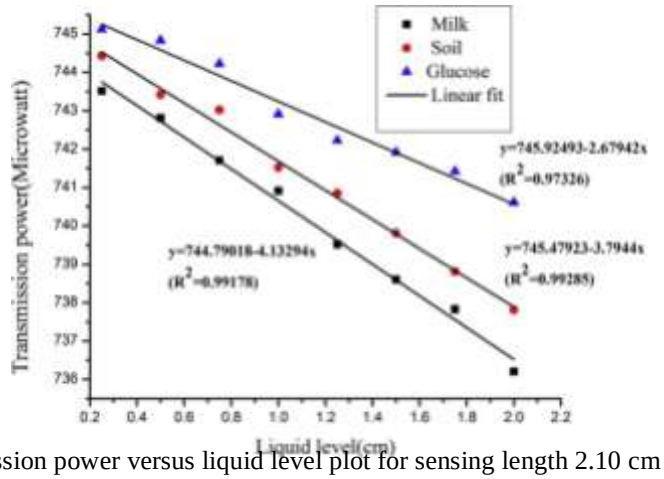

Fig. 12. Transmission power versus liquid level plot for sensing length 2.10 cm respectively with SMF–MMF–PCF–SMF structure.

liquids are turbid medium, it has characteristics of absorbance of light wave. Therefore, transmission power decreases with the increase of liquid level.

The linear fitted plots to transmission power versus liquid level of three different turbid mediums (milk, soil and glucose) are shown in Figs. 10–12 respectively for three sensing lengths (7.20 cm, 5.50 cm, 2.10 cm). The slopes of these lines measure the sensitivities of the devices for the three mediums, milk, soil, and glucose as 1.489 lw/cm, 1.197 lw/cm, and 1.032 lw/cm respectively for 7.2 cm PCF device, 9.098 lw/cm, 9.016 lw/cm, and 8.644 lw/cm respectively for 5.5 cm PCF device, and 4.133 lw/cm, 3.445 lw/cm, and 1.957 lw/cmrespectively for 2.1 cm PCF device. R^2 values of the fitted lines are 0.9. The results interpret relation between concentration of liquid and liquid level sensitivity. The sensitivity of this device decreases with increasing concentration as well as turbidity of liquid.

IV. CONCLUSIONS

In the present work, a new method is introduced to prove inter-ferometric nature of the simple in-line Mach–Zehnder interfero-metric sensor device at monochromatic wavelength. Moreover, this fabricated device shows sharp intensity deviation due to exter-nal parameters. The devices exhibit refractive index sensitivity in decreasing manner with increasing sensing length. Furthermore, the three fabricated devices exhibit as liquid level sensor for milk, soil, and glucose turbid medium. As liquid level sensitivity of the device decreases with increasing concentration of liquid, the sen-sor can be used to sense various optical properties like turbidity, absorbance, and transmittance of liquid. The fiber sensor can also detect the refractive index by monitoring the sensitivity of the device to the liquid level. Thus, a sensing device is proposed which can be used in sensing of other biological and chemical parameters.

REFERENCES

[1] A.D. Kersey, A review of recent developments in fiber optic sensor technology, Opt. Fiber Technol. 2 (36) (1996) 291–317.

[2] B.H. Lee, Y.H. Kim, K.S. Park, J.B. Eom, Interferometric fiber optic sensors, Sensors 12 (2012) 2467–2486.

[3] J. Mathew, Y. Semenova, G. Farrel athew, J. Semenova, Y. Rajan, G. Farrel, Humidity sensor based on a photonic crystal fiber interferometer, Electron. Lett. 46 (19) (2010) 1341–1343.

[4] L.V. Nguyen, D. Hwang, S. Moon, D.S. Moon, Y. Chung, High temperature fiber sensor with high sensitivity based on core diameter mismatch, Opt. Express 16 (15) (2008) 11369–11375.

[5] L. Li, L. Xia, All-fiber Mach–Zehnder interferometers for sensing applications, Opt. Express 20 (10) (2012) 11109–11120.

[6] H. Gong, H. Song, X. Li, J. Wang, X. Dong, An optical fiber curvature sensor based on photonic crystal fiber modal interferometer, Sens. Actuators, A 195 (2013) 139–141.

[7] J. Zhou, C. Liao, Y. Wang, G. Yin, X. Zhong, K. Yang, B. Sun, G. Wang, Z. Li, Simultaneous measurement of strain and temperature by employing fiber Mach–Zehnder interferometer, Opt. Express 22 (2) (2014) 1680–1686.

[8] Z. Cao, Z. Zhang, X. Ji, T. Shui, R. Wang, C. Yin, S. Zhen, L. Lu, B. Yu, Strain-insensitive and high temperature fiber sensor based on a Mach–Zehnder modal interferometer, Opt. Fiber Technol. 20 (1) (2014) 24–27.

[9] L. Xia, L. Li, W. Li, T. Kou, D. Liu, Novel optical fiber humidity sensor based on a no-core fiber structure, Sens. Actuators, A 190 (2013) 1–5.
[10] H.Y. Choi, M.J. Kim, B.H. Lee, All-fiber Mach–Zehnder type interferometers formed in photonic crystal fiber, Opt. Express 15 (9) (2007) 5711–5720.
[11] B. Larrión, M. Hernáez, F.J. Arregui, J. Goicoechea, J. Bravo, I.R. Mat´ıas, Photonic crystal fiber temperature sensor based on quantum dot nanocoatings, J. Sens. (Hindawi Publishing Corporation) 2009 (2009).
[12] Y. Yu, X. Li, X. Hong, Y. Deng, K. Song, Y. Geng, H. Wei, W. Tong, Some features of the photonic crystal fiber temperature sensor with liquid ethanol filling, Opt. Express 18 (15) (2010) 15383–15388.
[13] L.T. Hsiao, C.P. Yu, Mach–Zehnder fiber interferometers based on liquid-filled photonic crystal fibers, in: IEEE, 21st Annual Wireless and Optical Communications Conference (WOCC), 2012.
[14] J.N. Wang, J.L. Tang, Photonic crystal fiber Mach–Zehnder interferometer for refractive index sensing, Sensors 12 (2012) 2983–2995.
[15] R. Jha, J. Villatoro, G. Badenes, V. Pruneri, Refractometry based on a photonic crystal fiber interferometer, Opt. Lett. 34 (5) (2009) 617–619.
[16] B. Bourliaguet, C. Paré, F. Émond, A. Croteau, Microstructured fiber splicing, Opt. Express 11 (25) (2003) 3412–3417.
[17] L. Xiao, M.S. Demokan, W. Jin, Y. Wang, C.L. Zhao, Fusion splicing photonic crystal fibers and conventional single-mode fibers: microhole collapse effect, IEEE J. Lightwave Technol. 25 (11) (2007) 3563–3574.
[18] K. Borzycki, K. Schuster, Arc fusion splicing of photonic crystal fibers, in: Alessandro Massaro (Ed.), Photonic Crystals – Introduction, Applications and Theory, Intech, China, 2012, pp. 175–200.
[19] G. Coviello, V. Finazzi, J. Villatoro, V. Pruneri, Thermally stabilized PCF-based sensor for temperature measurements up to 1000 LC, Opt. Express 17 (24) (2009) 21551–21559.
[20] M.R. Shenoy, S.K. Khijwania, A. Ghatak, B.P. Pal, Fiber optics through experiments, second ed., Viva Book, 2009.
[21] S.S. Mishra, V.K. Singh, Study of non-linear properties of hollow core photonic crystal fiber, Optik 122 (2011) (2010) 687–690.
[22] Prerana, M.R. Shenoy, B.P. Pal, B.D. Gupta, Design, analysis, and realization of a turbidity sensor based on collection of scattered light by a fiber-optic probe, IEEE Sens. J. 12 (1) (2012) 44–50.